Time-lapse analysis using the wave-equation time migration

Alexandre W. Camargo, Tiago A. Coimbra, and Jorge H. Faccipieri

High-Performance Geophysics (HPG) Lab, Center for Energy and Petroleum Studies (CEPETRO), University of Campinas (UNICAMP), Brazil

This paper was prepared for presentation during the 18th International Congress of the Brazilian Geophysical Society, held in Rio de Janeiro, Brazil, 16-19 October, 2023.

Abstract

Imaging methods in the time-migration domain often rely on less accurate velocity models than those in the depth domain. This study proposes a wave-type equation approach to derive Reverse Time Migration (RTM) and Full-Waveform Inversion (FWI) methods in the time-migration domain. We start from the wave equation and derive the imaging condition from the adjoint equation, which enables us to perform an iterative least-square RTM or FWI, depending on the context. We also modify the image operator in the inversion method to update the velocity model in time. Based on synthetic data and a time-lapse case, our results reveal changes in the simulated reservoir and demonstrate the feasibility of these imaging techniques as alternatives to seismic processing in the depth-migration domain. In addition to being a new feature to be considered in seismic processing in the time-migration domain.

Introduction

Seismic imaging methods are essential tools for the oil and gas exploration industry. One of the most important is the time-lapse analysis, which involves conducting repeated seismic surveys of the same site at different times during reservoir exploitation (Lumley, 2001). However, conventional methods such as traveltime tomography or vertical seismic profile (Kasahara and Hasada, 2017) for quantifying time-lapse seismic effects often rely on an average-velocity wave propagation assumption that may not hold in real-world scenarios, leading to inaccurate results. Therefore, more sophisticated methods are necessary to capture time-lapse changes accurately. Besides, the unappropriated use of this assumption can lead to inaccurate time-domain images, especially when converted to depth in complex geological settings. Therefore, in order to obtain reliable images, more robust algorithms for imaging in the time domain are necessary for time-lapse analysis techniques in such situations.

We can use two powerful tools in the depth domain to accomplish images more suitable in the time domain: full-waveform inversion (FWI) and reverse-time migration (RTM). They aim to obtain a suitable depth image of the subsurface after several processing streams of the seismic dataset (Ikelle and Amundsen, 2018). However, these depth-domain methods require an initial velocity model with substantial accuracy (Symes, 2007; Glogovsky et al., 2009; Fichtner, 2011; Poliannikov and Malcolm, 2016). Indeed, an initial velocity model with few uncertainties implies the subsurface image obtained in the depth domain will present high-resolution quality. On the other hand, the traditional time-domain images are less sensitive to the velocity model that meets the needs of performing seismic interpretation to characterize the arrival time, amplitude, and slopes (Özdoğan Yilmaz, 2001; Fomel, 2014). These explain why time-domain methods are still relevant and substantially contribute to seismic exploration.

Time-migrated domain analyses are the first approach in seismic exploration, enabling the initial velocity construction for a suitable time-to-depth conversion. One of the central concepts in time-migrated domain methods is the image ray introduced by Hubral (1977). In summary, this concept states among all raypaths from a depth point to the measurement surface, the stationary time is when the phase vector of one of these rays arrives orthogonally to the observation surface, which we call an image ray, providing a way to obtain a relationship between the time and depth coordinates (Coimbra et al., 2023).

In recent years, many works have studied the time-to-depth conversion models (see, e.g., Cameron et al., 2007; Li and Fomel, 2014). Even though they are less sensitive to the velocity model requirements, the time-domain methods suffer in the presence of lateral velocity changes due to the geometric spreading factor. However, this limitation does not interfere when analyzing the time-domain imaging over seismic surveys taken at different times, i.e., time-lapse analysis.

Therefore, to perform a more reliable time-lapse analysis in the time-migration domain, we derived an adjoint equation associated with an acoustic wave-type equation that operates on the coordinates of the time-migration domain, called wave-equation time migration (Fomel and Kaur, 2021). In addition, we constructed an operator in such coordinates to perform FWI and create an input velocity for imaging via RTM in the same coordinates. Through this approach, we obtain a more robust method than conventional Kirchhoff time migration or other time-domain imaging methods that make use of an average velocity.

Method

The acoustic wave equation that governs the 2D phenomenon physical in exploration seismic (forward modeling) is given by

$$\mathscr{L}[v]u_S(t,x,z) = -f(t)\delta(x-x_S)\delta(z-z_S)\,, \tag{1}$$

where (x,z) is distance-depth coordinates, (x_S, z_S) is the source coordinates, t is the time, $f(t)$ is a temporal source function, $\delta(\cdot)$ is the Delta function, $v = v(x,z)$ is the wave velocity propagation function, $u_S(t,x,z)$ is the scalar wave response, and $\mathscr{L}[v]$ is the d'Alembert operator, namely

$$\mathscr{L}[v] = \frac{1}{v^2(x,z)}\frac{\partial^2}{\partial t^2} - \frac{\partial^2}{\partial x^2} - \frac{\partial^2}{\partial z^2}\,. \qquad (2)$$

Starting from an Eikonal-type equation based on changing coordinates from depth to time domain, Fomel and Kaur (2021) derive a 2D wave-equation time migration as

$$\hat{\mathscr{L}}[v_d]\hat{u}_S(t,\xi,\tau) = -f(t)\delta(\xi-\xi_0)\delta(\tau)\,, \qquad (3)$$

where (ξ,τ) is distance-traveltime coordinates, $(\xi_0, \tau_0 = 0)$ is the source-type coordinates, $v_d = v_d(\xi,\tau)$ is Dix velocity function (Dix, 1955), $\hat{u}_S(t,\xi,\tau)$ is the scalar wave-equation time migration response, and in this sense, the time-domain operator corresponds is

$$\hat{\mathscr{L}}[v_d] = \frac{1}{v_d^2(\xi,\tau)}\left(\frac{\partial^2}{\partial t^2} - \frac{\partial^2}{\partial \tau^2}\right) - \frac{\partial^2}{\partial \xi^2}\,. \qquad (4)$$

Coimbra et al. (2023) presents a significant contribution to the field of 3D wave-equation time migration by introducing a general anisotropic version of the Eikonal-type equation. This groundbreaking work opens new possibilities for modeling wave-type propagation in anisotropic media. Building upon their findings, future researchers can apply this methodology to various anisotropic media, expanding our understanding of wave behavior in complex geological structures.

Furthermore, we can see similar properties with the acoustic wave equation in the depth-domain coordinate. Thus, we can deduce the image operators in the time domain in the same way as found for the equation in depth. Accordingly, with variational calculus aid followed by Plessix (2006). Therefore, since the problem is hyperbolic, then the operator is self-adjoint. From that, the adjoint operator can be obtained and is given by

$$\hat{\mathscr{L}}^\dagger[v_d] = \hat{\mathscr{L}}[v_d]\,; \qquad (5)$$

where can we take

$$\hat{\mathscr{L}}^\dagger[v_d)]\hat{u}_{Ri}(t,\xi,\tau) = F_i^\dagger(t,\xi,\tau)\,, \qquad (6)$$

with $\hat{u}_{Ri}$ as the wave field generated by the back-propagation of the receivers that were records of the source (x_S, z_S) position and $F_i^\dagger$ is the source of the attached equation, $i = 1$ for RTM or $i = 2$ for FWI.

The image operators that use the full equation are RTM and FWI. Equation (6) generally governs both methods. The difference occurs in the term of the source, i.e., in RTM, the adjoint source corresponds to

$$F_1^\dagger(t,\xi,\tau) = \sum_{R=1}^{N_R}\delta(\xi - x_R)\delta(\tau-\tau_R)d(t_*-t, x_R, z_R; x_S, z_S)\,, \qquad (7)$$

where (x_R, z_R) is the receiver position coordinates, $\tau_R = z_R/v(x_R,z_R)$, N_R is the total number of receivers, t_* is the maximum time record, and $d(t,x_R,z_R;x_S,z_S)$ is the observed data. In real cases, such data is obtained from a seismic acquisition. However, for controlled analysis purposes, the data is simulated in the depth domain using a simulated model assumed to be the true velocity model, i.e., by simulating Equation (1). Besides, for FWI, the adjoint source depends on the choice of the misfit functional operator. Using the L^2-norm (Tarantola, 1984) we have

$$F_2^\dagger(t,\xi,\tau) = \sum_{R=1}^{N_R}\delta(\xi - x_R)\delta(\tau-\tau_R)\Delta d(t,\xi,\tau)\,, \qquad (8)$$

where

$$\Delta d(t,\xi,\tau) = d(t_*-t, x_R, z_R; x_S, z_S) - \hat{u}_S(t_*-t,\xi,\tau)\,. \qquad (9)$$

Therefore, with the appropriate adjoint sources, we have the migration and inversion using the wave equation operator in the time-migration domain.

Furthermore, the seismic image is obtained by applying the image condition. For the time-domain operator, we have

$$m_{S_i}(\xi,\tau) = \int_0^{t_*}\left(\frac{\partial^2\hat{u}_S}{\partial t^2} - \frac{\partial^2\hat{u}_S}{\partial \tau^2}\right)\hat{u}_{Ri}\,\mathrm{d}t\,, \qquad (10)$$

where for simplicity, we leave implicit the dependency of time-migration coordinates. Furthermore, we get the final image, m_I, by stacking all images, such as

$$m_I(\xi,\tau) = \sum_{S_1=1}^{N_S} m_{S_1}(\xi,\tau)\,. \qquad (11)$$

Finally, in the case of inversion, the seismic velocity is updated by gradient direction, i.e.,

$$\Delta v_d(\xi,\tau) = -\frac{2}{v_d(\xi,\tau)^3}\sum_{S_2=1}^{N_S} m_{S_2}(\xi,\tau)\,. \qquad (12)$$

Time-Lapse analysis comments

Seismic imaging through time-lapse monitoring offers a robust solution for managing and monitoring reservoirs by detecting changes in the subsurface over time (Hicks et al., 2016). However, it poses several challenges, especially in terms of dataset regularization. As reservoir geology becomes more complex and monitor fields differ from the baseline, it is crucial to ensure that the areas are equalized before implementing current seismic imaging methods. To achieve this, current regularization methods can be applied to baseline and monitor seismic-response datasets (e.g., Liu and Sacchi, 2004; Coimbra et al., 2016; Camargo et al., 2021, in prestack dataset). Even after regularization, there can still be significant differences between the fields, which can lead to errors in the imaging process. This can be especially problematic in intricate geological settings, where even minor subsurface changes can severely affect production and reservoir management. Therefore, it is imperative to address these challenges to ensure the effectiveness of seismic imaging techniques.

Results

To investigate the usability of velocity analysis, we tested on the synthetic model that is a length of 3 km and 2.1 km in depth, which has a uniform mesh of 6 m as shown in

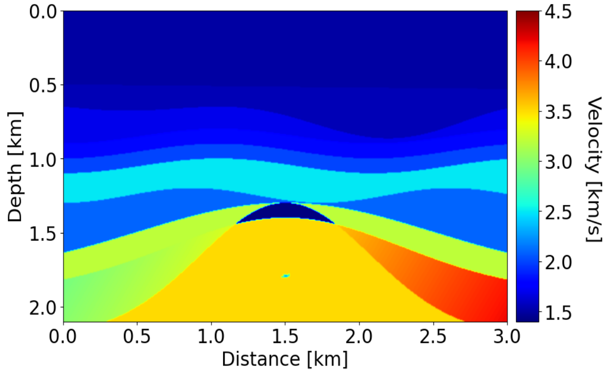

Figure 1: Velocity model in the depth domain.

Figure 1. The top of the dome is a representation of a reservoir with a seismic velocity of 1.4 km/s within.

The observed data were simulated by the finite-difference method using an operator of the second order in time and fourth order in space for an acoustic wave equation with *c-pml* absorbing condition (Komatitsch and Martin, 2007) and with source dominance frequency of 20 Hz. The data set consists of 126 shots taken from common-shot gathers. The shots are distributed uniformly at each 24 m on the model surface $(z = 0)$. Two hundred fifty-one receivers collected the records arranged every 12 m for a total time of 2 s. Figure 2 shows two shot gathers at 240 m and 1464 m.

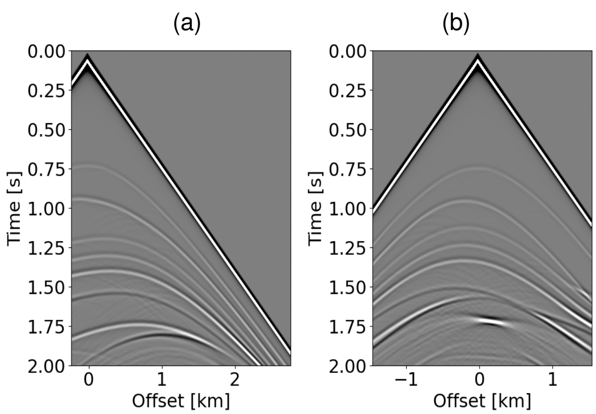

Figure 2: Common-shot gather for baseline seismic model located at (a) 240 m, and (b) 1464 m.

After assuming a producing reservoir, new acquisitions are performed over time. As part of this process, we simulate the injection of fluids into the reservoir, which can lead to changes in the physical properties of the rock and, with it, to changes in wave propagation velocity. We have constructed four monitor fields for this experiment that we will closely observe and analyze.

To extract an initial time-migration velocity with reasonable accuracy for later use in the migrated images of the base and monitor field, we use a time-migration coordinate construction based on the 1D model shown in Equation (13) and for lateral distance, we take $\xi = x$.

$$\tau(\xi) = \int_0^{z_*} \frac{dz}{v(x=\xi, z)}. \tag{13}$$

After this change of coordinates, we use a centered moving average filter with size 5×5 samples repeating one-thousand times to generate a smooth-velocity model. Figure 3 illustrates the seismic initial time velocity.

After ten iterations using the Conjugate-Gradient (CG) method without any regularization function, Figure 4 displays the obtained velocity-in-time model. The FWI technique resulted in an expected increase in resolution in most parts of the model. However, the absence of a long offset led to low-quality estimates of velocity and reflectivity at depths greater than 900 m. The normalized convergence history of the misfit function and the L2-norm gradient (see, Figure 5), i.e., the closer to zero better, exhibited the same behavior as the FWI in the depth domain.

For time-lapse analysis, we consider changing only the reservoir properties. We made four models, changing 25%, 50%, 75%, and 100% of the reservoir characteristics in the horizontal direction. We inserted a negative velocity gradient from left to right to simulate a gas injection in the reservoir. These models simulated the new seismic surveys, converted the velocity model to time, and performed migration and inversion analysis in the time domain.

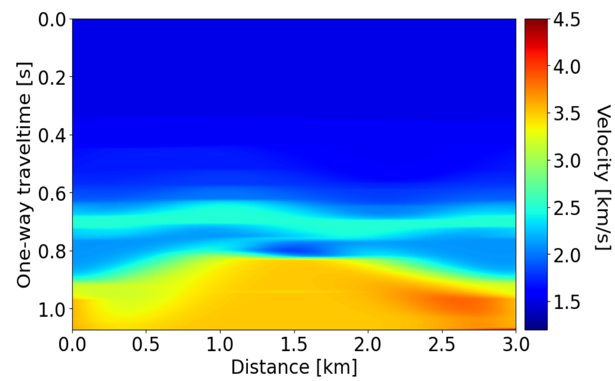

Figure 3: Initial velocity for migration velocity estimation using inversion with the proposed time-domain operator.

Figure 6(a) shows the migrated image using initial smooth velocity, and Figure 6(b) ones with the final FWI velocity for the base field model. The difference is insignificant, and there is more amplitude change than time shift, as observed in Figure 6(c).

Figures 7(a) to 7(d) show the migrated image of the four monitor fields. From these results, we observe a change of amplitude at the base of the reservoir due to the physical property shift from oil to gas, even if it is a smooth variation. In this case, we assumed that the water velocity did not vary over time, so we did not observe a time shift as may happen in real scenarios. To better observe the differences with the baseline model, the Figures 8(a) to 8(d) show the subtraction of the migrated image from the monitor model with the baseline model. Note that the time evolution also captures changes below the reservoir because the transmission and reflectivity of the material are different.

The seismic data from each monitor was analyzed to determine changes in the reservoir. The FWI was utilized with the velocity obtained from the previous time-lapse to

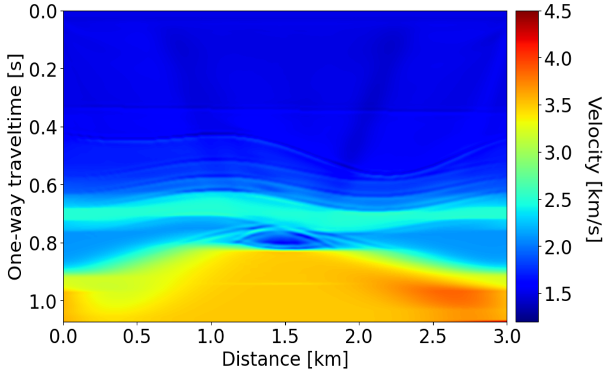

Figure 4: FWI estimated velocity in time domain.

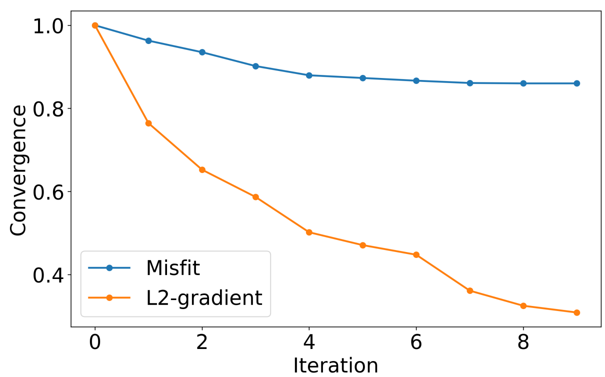

Figure 5: Convergence history of CG method.

perform this analysis. The reference velocity obtained from the baseline field was used for monitor one, while the output of the FWI applied from monitor one was used for monitor two, and so on. The differences from the baseline velocity were calculated to progress forward, as shown in Figures 9(a) to 9(d). The intensity of the differences decreases with each time-lapse as the velocity decreases.

Conclusions

This work proposes a novel approach to deriving RTM and FWI imaging techniques using the wave-type equation operator in the time-migration domain. The advantage of this approach is that velocity-time analysis requires less precision than depth analysis, which makes it easier to estimate initial models in time. Our testing shows that both the RTM and FWI techniques are viable in detecting changes in amplitude and velocity during time-lapse analysis to monitor reservoir characterization. These changes can be attributed to the improved accuracy of the velocity model, which has important implications for various applications, such as oil and gas exploration and environmental monitoring. Our findings demonstrate that the proposed imaging techniques provide a valuable alternative to seismic processing in the time-migration domain. By using the operators, we can derive imaging techniques that are more accurate and effective, particularly in monitoring reservoir characterization over time. Therefore, this work has significant implications for improving the accuracy and efficiency of imaging methods in seismic processing.

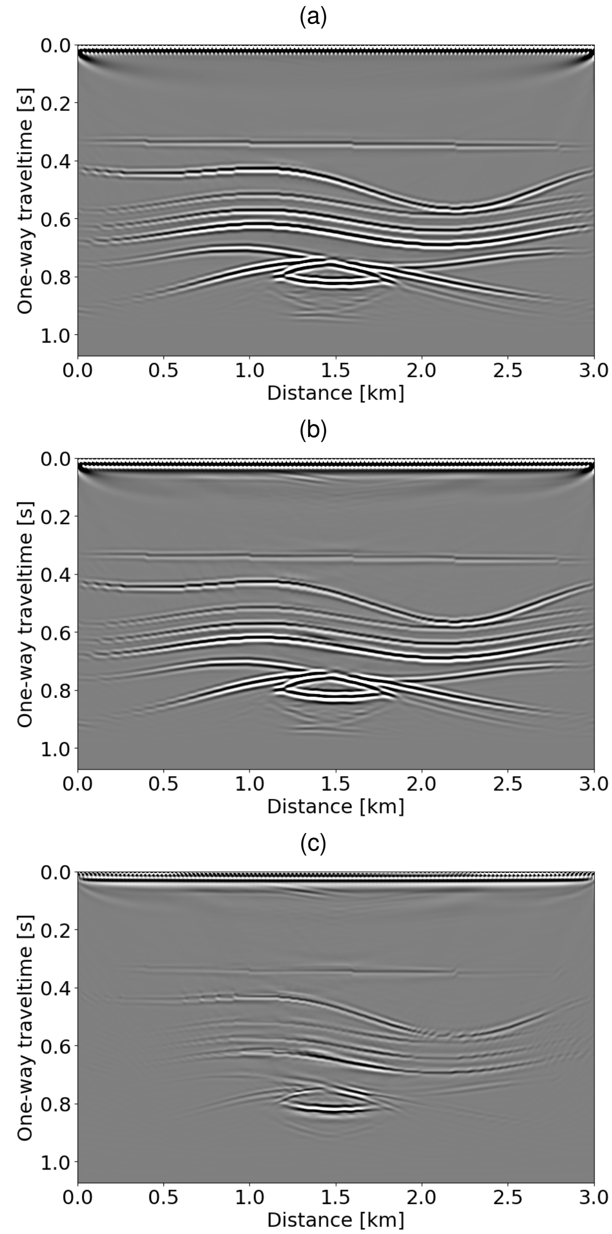

Figure 6: Migrated image for Baseline fields using velocity migration. (a) Initial smooth velocity, (b) Output time operator FWI, and (c) Difference.

Acknowledgments

The authors thank the High-Performance Geophysics (HPG) team for technical support. This work was possible thanks to the support of Petrobras.

References

Camargo, A. W., J. Ribeiro, T. Coimbra, G. Ignácio, and M. Tygel, 2021, Offset-continuation-trajectory (OCT) data regularization to a 2d ocean bottom node (OBN): Full-wave inversion application: Brazilian Journal of Geophysics, **39**, 125–138.

Cameron, M. K., S. B. Fomel, and J. A. Sethian, 2007, Seismic velocity estimation from time migration: Inverse Problems, **23**, 1329–1369.

Coimbra, T. A., R. Bloot, and J. H. Faccipieri, 2023, Exploring velocity-spreading factor and consequences through dynamic ray-tracing in general anisotropic media: A comprehensive tutorial: ArXiv.org, **2304**.

Coimbra, T. A., A. Novais, and J. Schleicher, 2016, Offset-continuation stacking: Theory and proof of concept: Geophysics, **81**, V387–V401.

Dix, C. H., 1955, Seismic velocities from surface measurements: Geophysics, **20**, 68–86.

Fichtner, A., 2011, Full seismic waveform modeling and inversion: Springer. Advances in Geophysical and Environmental Mechanics and Mathematics.

Fomel, S., 2014, Recent advances in time-domain seismic imaging: Presented at the SEG Technical Program Expanded Abstracts 2014, Society of Exploration Geophysicists.

Fomel, S., and H. Kaur, 2021, Wave-equation time migration: Geophysics, **86**, S103–S111.

Glogovsky, V., E. Landa, S. Langman, and T. Moser, 2009, Validating the velocity model: the hamburg score: First Break, **27**.

Hicks, E., H. Hoeber, M. Houbiers, S. P. Lescoffit, A. Ratcliffe, and V. Vinje, 2016, Time-lapse full-waveform inversion as a reservoir-monitoring tool — a north sea case study: The Leading Edge, **35**, 850–858.

Hubral, P., 1977, Time migration – Some ray theoretical aspects: Geophysical Prospecting, **25**, 738–745.

Ikelle, L. T., and L. Amundsen, 2018, Introduction to petroleum seismology: Society of Exploration Geophysicists, volume **1** *of* Investigation in geophysics N.12.

Kasahara, J., and Y. Hasada, 2017, Time lapse approach to monitoring oil, gas, and CO2 storage by seismic methods: Elsevier.

Komatitsch, D., and R. Martin, 2007, An unsplit convolutional perfectly matched layer improved at grazing incidence for the seismic wave equation: Geophysics, **72**, SM155–SM167.

Li, S., and S. Fomel, 2014, A robust approach to time-to-depth conversion and interval velocity estimation from time migration in the presence of lateral velocity variations: Geophysical Prospecting, **63**, 315–337.

Liu, B., and M. D. Sacchi, 2004, Minimum weighted norm interpolation of seismic records: GEOPHYSICS, **69**, 1560–1568.

Lumley, D. E., 2001, Time-lapse seismic reservoir monitoring: Geophysics, **66**, 50–53.

Özdoğan Yilmaz, 2001, Seismic data analysis: Processing, inversion and interpretation of seismic data: Society of Exploration Geophysicists, volume **1** *of* Investigation in geophysics.

Plessix, R.-E., 2006, A review of the adjoint-state method for computing the gradient of a functional with geophysical applications: Geophysical Journal International, **167**, 495–503.

Poliannikov, O. V., and A. E. Malcolm, 2016, The effect of velocity uncertainty on migrated reflectors: Improvements from relative-depth imaging: Geophysics, **81**, S21–S29.

Symes, W. W., 2007, Reverse time migration with optimal checkpointing: Geophysics, **72**, SM213–SM221.

Tarantola, A., 1984, Inversion of seismic reflection data in the acoustic approximation: Geophysics, **49**, 1259–1266.

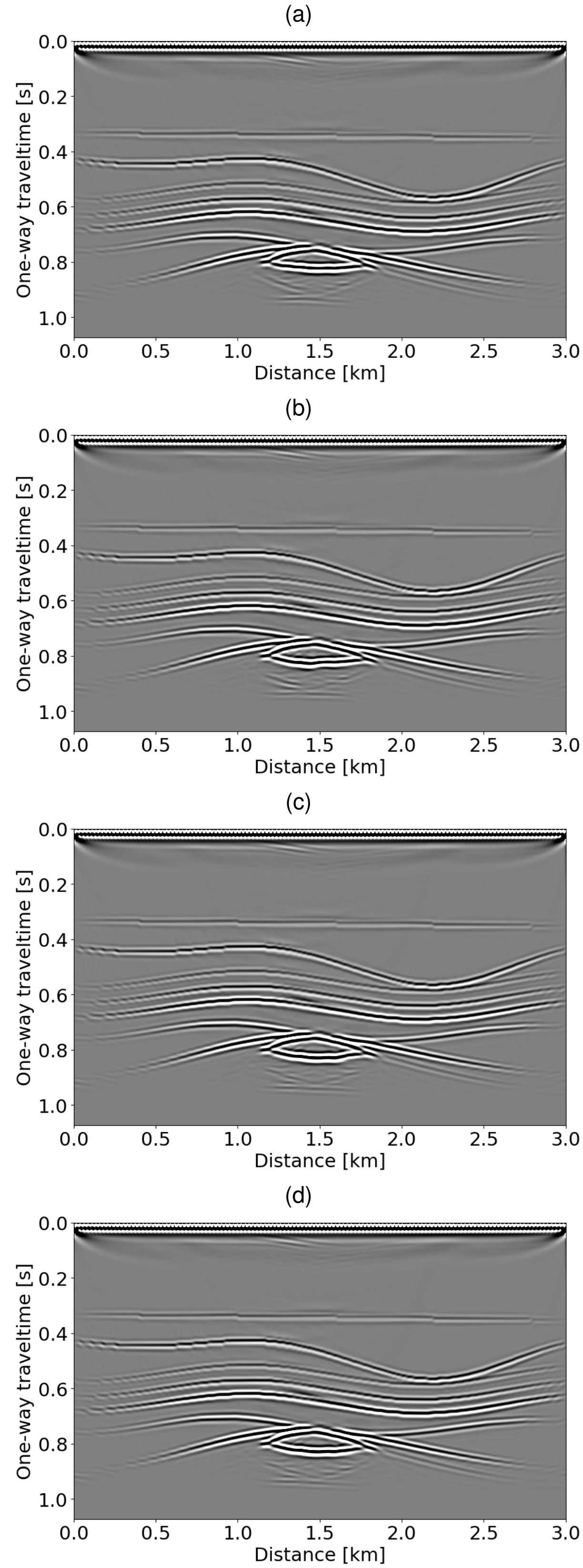

Figure 7: Migrated image fields. (a) Monitor 1; (b) Monitor 2; (c) Monitor 3; (d) Monitor 4.

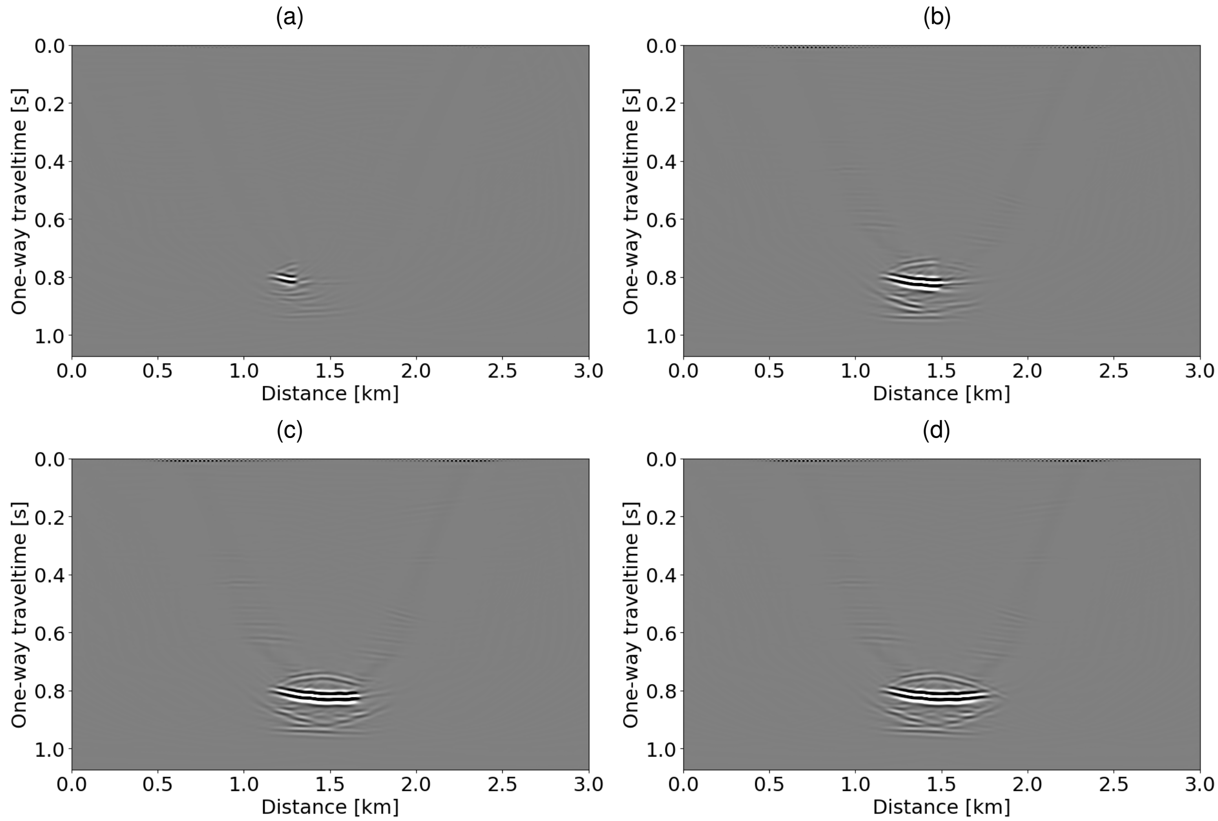

Figure 8: Difference with relation to Baseline field. (a) Monitor 1; (b) Monitor 2; (c) Monitor 3; (d) Monitor 4.

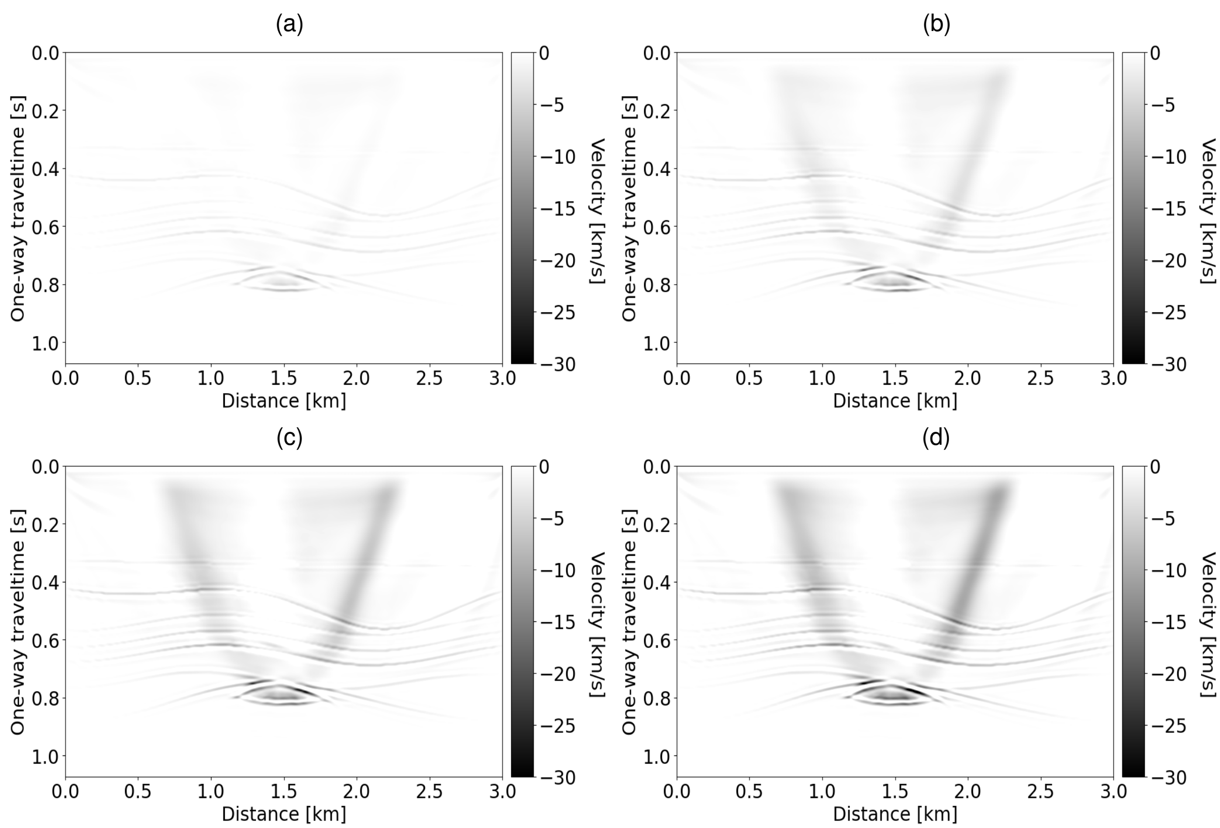

Figure 9: FWI Difference with relation to Baseline field. (a) Monitor 1; (b) Monitor 2; (c) Monitor 3; (d) Monitor 4.